

JNM

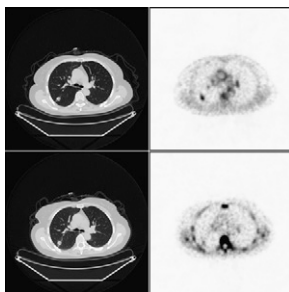
Combining optical and nuclear imaging: Culver and colleagues provide a molecular imaging focus on the current status of multimodality applications fusing PET or SPECT with optical techniques in small-animal and clinical studies. . . . *Page 169*

Sudden arrhythmic cardiac death: Travin assesses the role for radionuclide imaging approaches in prediction and prevention of death resulting from ventricular arrhythmia, including the potential for management benefits in patients with implantable cardioverter defibrillators. . . . *Page 173*

Resolving ¹²³I-ADAM neuroimaging questions: Slifstein reviews past discrepancies in modeling approaches for neuroimaging with the serotonin transporter radioligand ¹²³I-ADAM and previews a related article in this issue of *JNM*. . . . *Page 176*

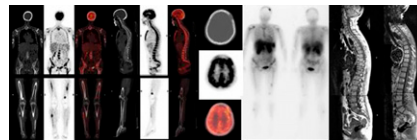
PET and CT accuracy in pulmonary nodules: Fletcher and colleagues report on a multiinstitutional study comparing the ability of PET and CT imaging to characterize solitary lung nodules in a population of military veterans. . . . *Page 179*

Dual-tracer PET/CT in lung nodules: Tian and colleagues describe the results of a clinical trial investigating the complementary capabilities of ¹⁸F-FDG and ¹⁸F-FLT in PET/CT imaging of pulmonary nodules. . . . *Page 186*

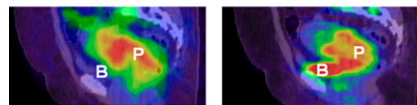


Optimal imaging strategies in multiple myeloma: Fonti and colleagues compare the contributions of ¹⁸F-FDG PET/CT, ^{99m}Tc-sestamibi scintigraphy, and MRI in whole-body

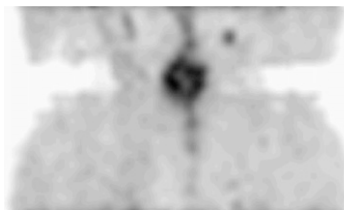
and regional evaluation of patients with newly diagnosed multiple myeloma. . . . *Page 195*



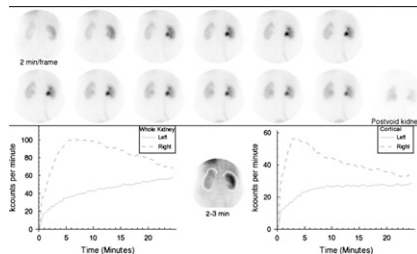
PET and tumor hypoxia: Dehdashti and colleagues report on the use of pretreatment ⁶⁰Cu-ATSM PET in assessing tumor oxygenation as a predictor of outcomes in patients with cervical cancer. . . . *Page 201*



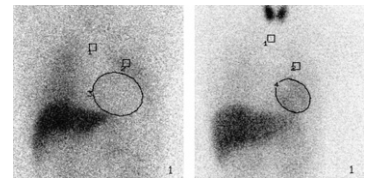
Prostate acetate kinetics: Schiepers and colleagues describe models of acetate kinetics in prostate cancer and discuss the potential benefits of ¹⁻¹³C-labeled acetate PET in staging and monitoring of the disease. . . . *Page 206*



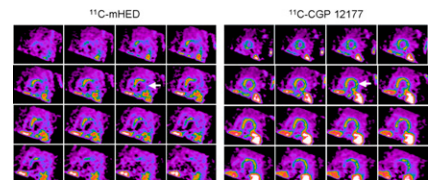
Automated assessment of renal obstruction: Taylor and colleagues compare diuresis renography interpretations generated by a renal expert system with those of 3 experienced readers and outline the utility of this tool for education and clinical decision support. . . . *Page 216*



Candidates for ICD: Nagahara and colleagues assess altered autonomic function, as measured by cardiac MIBG activity, as a partial predictor of fatal cardiac events and as a method for identifying patients who would benefit most from implantable cardioverter defibrillators. . . . *Page 225*

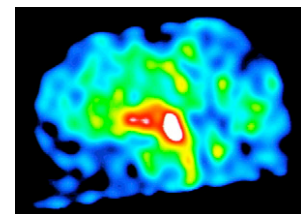


Sympathetic mismatch in ischemic CHF: Caldwell and colleagues describe research with PET imaging to determine whether a specific presynaptic-to-postsynaptic mismatch characterizes cardiac sympathetic function in ischemic congestive heart failure. . . . *Page 234*



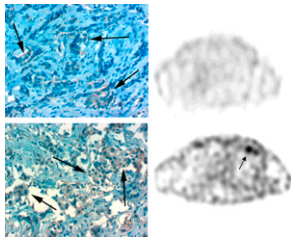
Abbreviating misery perfusion scans: Kobayashi and colleagues report on the development of a count-based method for shorter continuous inhalation in ¹⁵O-gas PET assessment of hemodynamic status in patients with ischemic cerebrovascular disease. . . . *Page 242*

Evaluation of ¹²³I-ADAM imaging: Frokjaer and colleagues explore several kinetic and semiquantitative methods for assessing serotonin transporter binding using ¹²³I-ADAM SPECT in humans. . . . *Page 247*



¹⁸F-galacto-RGD PET in breast cancer: Beer and colleagues elucidate the uptake patterns of this $\alpha_v\beta_3$ -selective PET tracer in patients with invasive ductal breast cancer and describe its potential utility in assessment of angiogenesis and in treatment planning. **Page 255**

GRP-receptor imaging in breast carcinoma: Van de Wiele and colleagues report on scintigraphic studies of ^{99m}Tc-RP527 uptake in human breast cancer as related to gastrin-releasing peptide receptor expression. **Page 260**

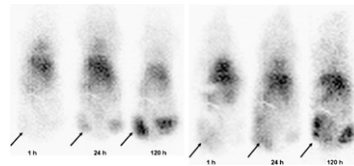


Uncommon causes of thyrotoxicosis: Mitra and colleagues offer an educational overview of the less common causes of elevated free thyroid hormones and provide illustrative patient cases as well as best-practice recommendations. . . . **Page 265**

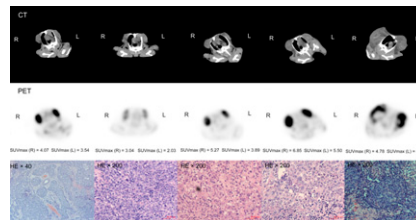
Marrow radionuclide dosimetry: Meredith and colleagues describe a novel method to correct for background radioactivity contributed from blood in large vessels that overlap the spine in image-based dosimetry of lumbar vertebrae. **Page 279**

In vivo microRNA imaging: Lee and colleagues detail the development of a dual-luciferase reporter system for monitoring in vivo transcription of microRNA activity. **Page 285**

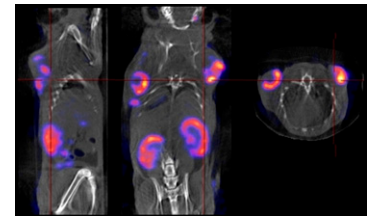
Pulsed HIFU and tumor mAb uptake: Khaibullina and colleagues explore the ability of pulsed high-intensity focused ultrasound to enhance uptake of a radiolabeled monoclonal antibody to human epidermoid tumor in a mouse model. **Page 295**



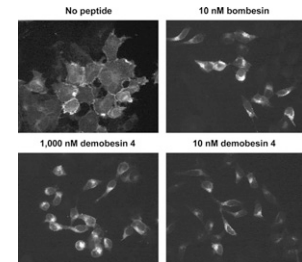
PET/CT and chemosensitivity: Song and colleagues investigate whether ¹⁸F-FDG PET/CT can be used for in vivo chemosensitivity testing and identify optimal time points for such imaging in cisplatin administration in rabbits with implanted squamous cell tumors. **Page 303**



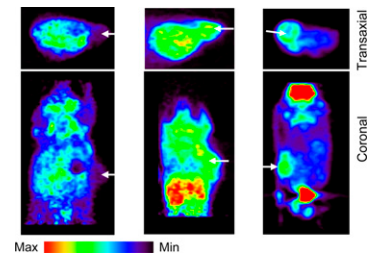
^{99m}Tc-His-folate SPECT/CT: Müller and colleagues report on SPECT/CT imaging of folate receptor-positive malignant and normal tissues and organs, including the salivary glands and choroid plexus, using an improved organometallic ^{99m}Tc-radiofolate. **Page 310**



Bombesin analogs in tumor targeting: Cescato and colleagues describe 2 bombesin analogs, a gastrin-releasing peptide receptor agonist and an antagonist, and assess their ^{99m}Tc-labeled ligands for in vitro and in vivo tumor-targeting properties. **Page 318**



^{1-¹¹C-acetate and FAS expression:} Vävere and colleagues evaluate the potential value of this tracer as a PET radiopharmaceutical for imaging fatty acid synthase expression in prostate cancer. **Page 327**



ON THE COVER

The integrin $\alpha_v\beta_3$, an interesting target for specific therapies in oncology, is highly expressed on activated endothelial cells during angiogenesis and plays an important role in the regulation of tumor growth, local invasiveness, and metastatic potential. As confirmed by the immunohistochemistry images, these ¹⁸F-galacto-RGD PET images of invasive ductal breast cancer show $\alpha_v\beta_3$ expression predominantly on the neovasculature.

See page 258.

